computing@computingonline.net
www.computingonline.net

ISSN 1727-6209
International Journal of Computing

POST-CORRECTION OF ADC NON-LINEARITY USING INTEGRAL NON-LINEATITY CURVE

Vladimir Haasz [1], David Slepicka [1], Petr Suchanek [2]

[1] Czech Technical University in Prague, Faculty of electrical Engineering, Technicka 2, 16627 Praha 6, Czech Republic, haasz@fel.cvut.cz, slepicd@fel.cvut.cz, http://measure.feld.cvut.cz
[2] Evolving systems consulting s.r.o., Čs. armády 14, 160 00 Praha 6, Czech Republic, petr.suchanek@evolvsys.cz

Abstract: *The accuracy of AD conversion can be improved using the post-correction of digitizer non-linearity. In principle two methods could be applied – look-up table or an analytical inverse function of integral non-linearity curve (INL(n)). Look-up table can be easily implemented but it demands huge memory space particularly for high resolution ADCs. Inverse function offers flexible solution for parameterization (e.g. frequency dependence) but it also requires fast DSP for real-time correction. The data or coefficients for both methods are frequently determined from a histogram of acquired pure sinusoidal signal. Non-linearity curve can also be gained by another procedure demanding significantly less samples – approximation from a frequency spectrum. The correction of ADC nonlinearity by means of inverse function of INL(n) curve is analyzed in this paper and the results are presented.*

Keywords: *analog-to-digital converter, ADC non-linearity, INL, transfer function, approximation, non-linearity correction, simulations, experimental verification.*

1. INTRODUCTION

The ADC non-linearity is inherently described by the Integral Non-linearity curve *INL*(*n*) which is defined as the difference of ADC output and input as the function of the input level. *INL*(*n*) can be directly determined using histogram method [1], but this method demands a huge number of samples in a record, thus it is time consuming. However, non-linearity causes also a distortion in the digitized signal and the frequency spectrum can provide similar information as the *INL*(*n*) in the code domain.

The *INL*(*n*) curve can be split into its low code frequency component (LCF) and the high code frequency component (HCF). The LCF (the rough curve of the *INL*(*n*)) – see Fig. 1, dotted curve) is responsible for harmonic distortion at lower harmonic components [2, 3, 4], usually the strongest are 2nd and the 3rd ones. If an approximation of the *INL*(*n*) curve using polynomials is applied, the third order polynomial is mostly sufficient for the following integral non-linearity correction.

2. APPROXIMATION OF *INL*(*N*) CURVE

Using polynomials the *INL*(*n*) is approximated by

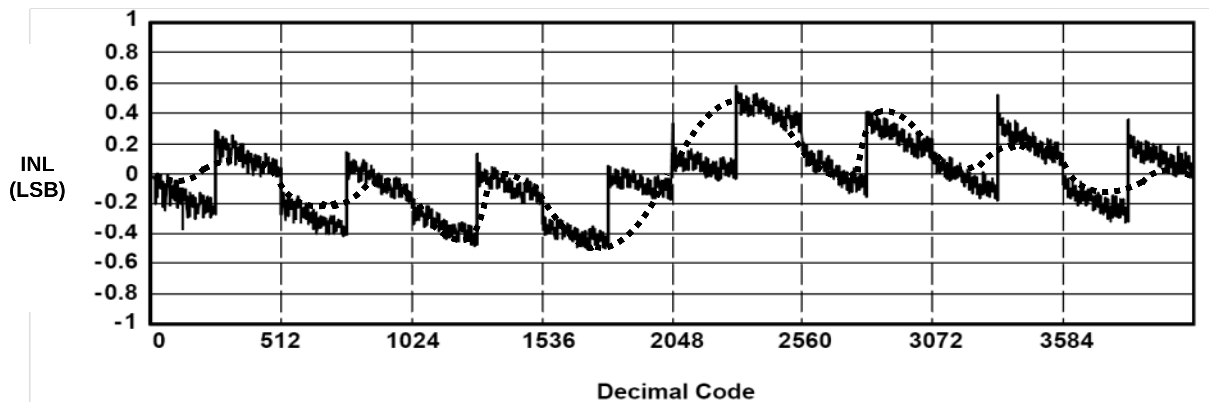

Fig. 1 – An example of *INL*(*n*) curve and its low code frequency component (dotted curve)

$$INL(n) = \sum_{h=1}^{H_{\max}} a_h x^h(n) \tag{1}$$

where a_h are the nonlinearity coefficients up to the maximum order $H_{\max}$, which is the highest harmonic component considered, n is the normalized ADC code with a bipolar range, and x the ADC input. Having the coefficients a_h and consequently the approximation of $INL(n)$ curve, the non-linearity of digitizer can be corrected. The approximated transfer function TF has to be calculated by adding a straight line to the $INL(n)$, such that

$$TF(n) = n + INL(n) \tag{2}$$

where n is the ADC code and after the substitution it can be expressed as

$$TF(n) = n + \sum_{h=1}^{H_{\max}} a_h x^h(n) \tag{3}$$

If the transfer function TF is monotonical, its inverse exists. For this case, let's propose that the approximation of the inverted transfer function TF^{-1} will also be a polynomial of the same order ($K_{max} = H_{max}$) defined as

$$TF^{-1}(y) = \sum_{k=1}^{K_{\max}} b_k y^k \tag{4}$$

where y is the ADC output. Substituting $y = TF(n)$ from (3) into (4)

$$\begin{aligned} TF^{-1}(TF(n)) &= \sum_{k=1}^{K_{\max}} b_k \left[TF(n)\right]^k = \\ &= \sum_{k=1}^{K_{\max}} b_k \left[\sum_{h=1}^{H_{\max}} a_h n^h\right]^k \end{aligned} \tag{5}$$

The distortion of the 2nd and the 3rd harmonic component is usually the most important for majority of digitizers and the higher components are usually negligible. Therefore the $K_{max} = H_{max} = 3$ will be taken into account for the following solution. In this case the general expression (5) changes to

$$\begin{aligned} TF^{-1}(TF(n)) &= \sum_{k=1}^{3} b_k \left[\sum_{h=1}^{3} a_h n^h\right]^k = \\ &= b_1(a_1 n + a_2 n^2 + a_3 n^3) + \\ &+ b_2(a_1 n + a_2 n^2 + a_3 n^3)^2 + \\ &+ b_3(a_1 n + a_2 n^2 + a_3 n^3)^3 \end{aligned} \tag{6}$$

Considering

$$TF^{-1}(TF(n)) = n \tag{7}$$

and comparing the coefficients of the same powers of n an over determined equation system arises (3 unknowns variables b_1, b_2, b_3, 9 equations).

Two methods for the determination of coefficient b_k are presented in this paper. In the first method the coefficients b_1, b_2, b_3 are determined from 3 low-order equations, the equations with polynomials n^l, $l > 3$ are neglected. The coefficients are given by

$$b_1 = \frac{1}{a_1}, \quad b_2 = \frac{a_2}{a_1^3}, \quad b_3 = \frac{2a_2^2}{a_1^5} - \frac{a_3}{a_1^4} \tag{8}$$

The second method is more sophisticated. Since equation (7) can hardly be fulfilled completely the error function

$$e = \left(TF^{-1}\left(TF(n)\right) - n\right)^2 \tag{9}$$

is minimized (least square).

Let's integrate the error function over the full-scale of the ADC to obtain the area below the error function. The full-scale range of the ADC spans over $\langle -1;+1 \rangle$ interval because of normalization.

$$I(b_1, b_2, b_3) = \int_{-1}^{+1} \left(TF^{-1}\left(TF(n)\right) - n\right)^2 dn \tag{10}$$

and after the substitution from (6)

$$\begin{aligned} I(b_1, b_2, b_3) = \int_{-1}^{+1} (&b_1(a_1 n + a_2 n^2 + a_3 n^3)^3 + \\ &+ b_2(a_1 n + a_2 n^2 + a_3 n^3)^2 + \\ &+ b_3(a_1 n + a_2 n^2 + a_3 n^3) - n)^2\, dn \end{aligned} \tag{11}$$

Integration (11) eliminates the variable n and only variables b_k remain. Let's take the partial derivatives of the $I(b_1,b_2,b_3)$ function with respect to three variables and equal them to zero.

$$\frac{\delta I}{\delta b_1} = 0, \quad \frac{\delta I}{\delta b_2} = 0, \quad \frac{\delta I}{\delta b_3} = 0 \tag{12}$$

The system with three equations of three variables is obtained

$$\begin{aligned} c_1 b_1 + c_2 b_2 + c_3 b_3 &= d_1 \\ c_4 b_1 + c_5 b_2 + c_6 b_3 &= d_2 \\ c_7 b_1 + c_8 b_2 + c_9 b_3 &= d_3 \end{aligned} \tag{13}$$

where c_i and d_j are collected terms resulting from the partial derivations (12), e.g.

$$c_1 = \frac{4}{3}a_1^2 + \frac{4}{5}a_2^2 + \frac{8}{5}a_1 a_3 + \frac{4}{7}a_3^2 \tag{14}$$

and

$$d_1 = \frac{4}{3}a_1 + \frac{4}{5}a_3 \tag{15}$$

The equations (13) can be rewritten into a matrix form

$$\mathbf{C}\ \mathbf{b} = \mathbf{d} \tag{16}$$

and the coefficients b_1, b_2, b_3 can be calculated by applying the Cramer's rule based on determinants

$$b_1 = \frac{\det(C_1)}{\det(C)}, \quad b_2 = \frac{\det(C_2)}{\det(C)}, \quad b_3 = \frac{\det(C_3)}{\det(C)} \tag{17}$$

The solution is

$$\begin{aligned} b_1 &= \frac{d_1 c_5 c_9 + d_2 c_8 c_3 + c_2 c_6 d_3 - c_3 c_5 d_3 - c_2 d_2 c_9 - d_1 c_6 c_8}{c_1 c_5 c_9 + c_4 c_8 c_3 + c_2 c_6 c_7 - c_3 c_5 c_7 - c_2 c_4 c_9 - c_1 c_6 c_8} \\ b_2 &= \frac{c_1 d_2 c_9 + c_4 d_3 c_3 + d_1 c_6 c_7 - c_3 d_2 c_7 - d_1 c_4 c_9 - c_1 c_6 d_3}{c_1 c_5 c_9 + c_4 c_8 c_3 + c_2 c_6 c_7 - c_3 c_5 c_7 - c_2 c_4 c_9 - c_1 c_6 c_8} \\ b_3 &= \frac{c_1 c_5 d_3 + c_4 c_8 d_1 + c_2 d_2 c_7 - d_1 c_5 c_7 - c_2 c_4 d_3 - c_1 d_2 c_8}{c_1 c_5 c_9 + c_4 c_8 c_3 + c_2 c_6 c_7 - c_3 c_5 c_7 - c_2 c_4 c_9 - c_1 c_6 c_8} \end{aligned} \tag{18}$$

3. SIMULATION OF NON-LINEARITY CORRECTION

The correction of the simulated ADC nonlinearity was performed in the second step. The coefficients of the polynomials of the approximated non-linearity *INL*(*n*) curve (1) were computed from the histogram method [1] measured by the digitizer NI PXI 5122. Spectrally pure (filtered) testing signal (THD < -130 dB) was used for this purpose [5]. The approximation of the inverted transfer function was found applying the polynomials. Only the most dominant coefficients a_i (the 2nd and the 3rd order) were considered.

The levels of harmonic components of the simulated output signal and of the same signal after the correction are presented in Table 1. The performance of both methods mentioned above is shown.

Table 1. Results of Correction

Harmonic component	Digital output before correction	Digital output after correction	
		Direct inversion	LSE minimization
2	–77dB	–131dB	–142dB
3	–80dB	–136dB	–155dB

The modeled input and corresponding output signal were in a very good agreement with the real signals. The correction applied on this signal showed to be very effective. However, the correction on real output data did not improve the signal as expected. The reason seemed to be in other ADC imperfections (additive noise, jitter in sampling, non-zero sampled signal phase and hysteretic behavior) which were not taken into account in the simulation. To find the source of the worse correction results in the case of real data further simulations were executed. The influence of the incoherently sampled signal (with non-zero α) was suppressed by applying the Blackman-Harris window of the 7th order to the recorded data. The simulated distorted ADC output was generated as

$$\mathrm{ADC}_{\mathrm{output}} = y = \sum_{h=1}^{3} \mathrm{sign}(\mathbf{a}(h)) \left[\mathrm{abs}\left(\frac{\mathbf{a}(h)}{\mathbf{a}(1)} \right) \mathrm{ADC}_{\mathrm{input}} \right]^h \tag{19}$$

where $\mathbf{a} = [adc\_full\_scale, -18, -13]$ ($adc\_full\_scale = 2^{23}$ for the simulated 23-bit ADC and the numbers –18 and –13 are the coefficients of the 2nd and the 3rd non-linearity order). No rounding (quantization in amplitude) of the ADC output was used in order to better observe the performance of the correction. The following ADC imperfections were added to the modeled output signal:

a) additive white noise,
b) sampling jitter,
c) influence of non-zero sampled signal phase,
d) hysteresis.

The result corresponding to harmonic distortion only was used as the reference one (Fig. 2). The influence of the additive noise is presented in Fig. 3.

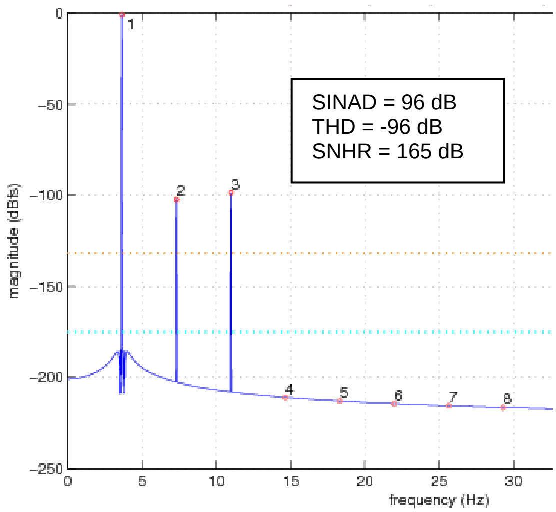

a) **Frequency spectrum before correction**

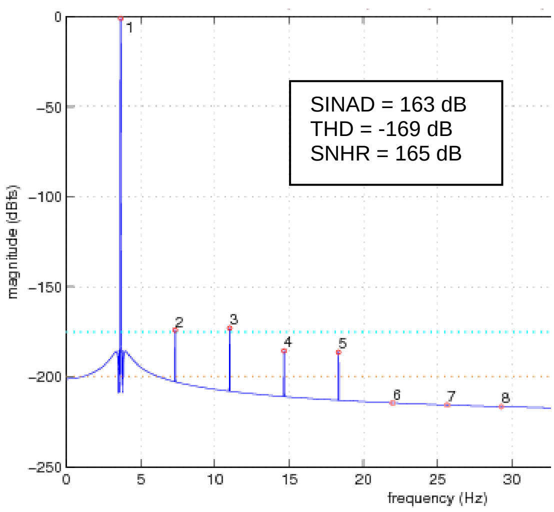

b) **Frequency spectrum after correction**

Fig. 2 – Non-linearity correction of simulated signal – sine-wave signal with harmonic distortion

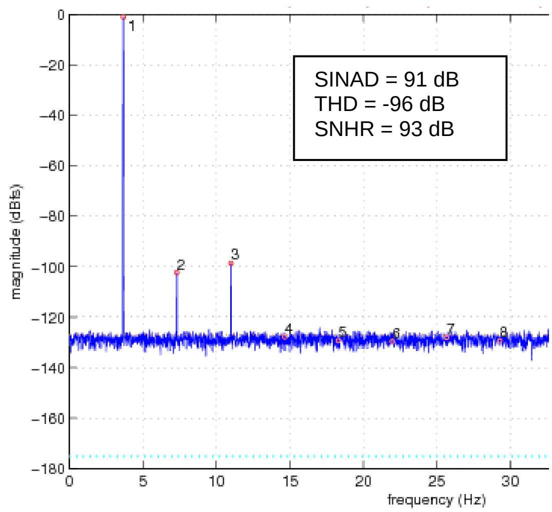

a) **Frequency spectrum before correction**

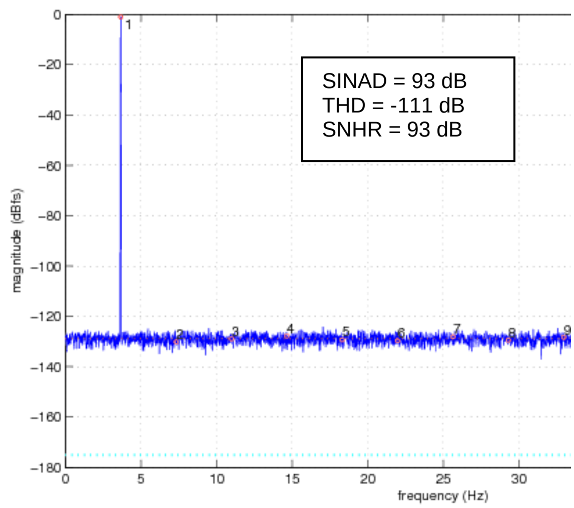

b) **Frequency spectrum after correction**

Fig. 3 – Non-linearity correction of simulated signal – sine-wave signal with white noise (σ^2 = 60 LSB) and harmonic distortion

This simulation proved that the presence of an additive white noise does not cause noticeably influence the results of correction – higher harmonic components were suppressed to negligible level below noise. The same result was found for sampling jitter. The simulation with variable non-zero sampled signal phase showed also no influence.

The last imperfection of a real ADC, which was investigated, was the hysteresis. For better observation the resulting frequency spectrum as well as the integral non-linearity curve (the deviation from the ideal transfer function – residual amplitude) were calculated (see Fig. 4).

The residual amplitude for falling and rising slopes was plotted individually. The dashed and dot-dash lines were reconstructed from the falling and rising slopes of the signal. *INLd* is so called "differential-mode" component which corresponds to ADC hysteresis behavior. The full line represents the "common-mode" non-linearity component *INLc* [6]. The hysteresis was modeled using equation

$$y^{\text{hyst}}(x) = \beta\left[\left(\frac{x}{X_1}\right)^2 - 1\right]\text{sign}(x'), \qquad (20)$$

where $y^{\text{hyst}}(x)$ is the additive contribution of the ADC hysteresis to its output, β is a the proportion factor, X_1 is the amplitude of the input signal, and the sign(x') is a binary function with +1 and –1 output values depending on the slope of the input signal x. Fig. 4c shows "typical" curves of residual amplitude, which is significantly different for failing and rising slopes.

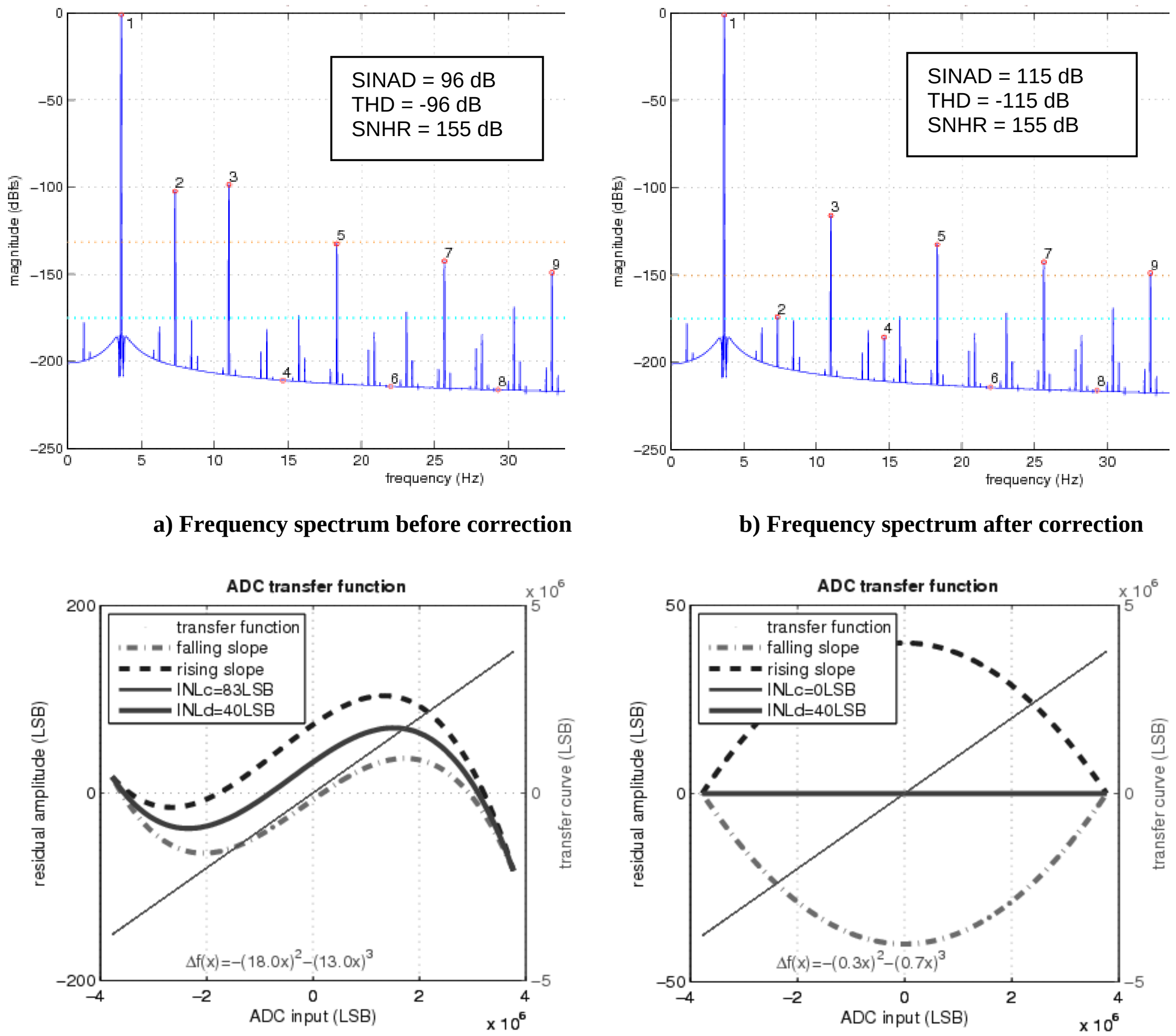

a) Frequency spectrum before correction

b) Frequency spectrum after correction

c) Transfer function before correction

d) Transfer function after correction

Fig. 4 – Non-linearity correction of simulated signal – sine-wave signal with hysteresis α = 40 LSB and harmonic distortion

The result of the correction is presented in Fig. 4d. The "common mode" non-linearity was correctly estimated as $\Delta f(x) = -(18.0x)^2 - (13x)^3$ LSB and removed. Only the hysteresis remained after the correction. It corresponds to the premise that the proposed method can correct only "pure" non-linearity, but not the hysteresis.

4. EXPERIMENTAL VERIFICATION

To verify the simulation results experimental measurements using two high quality digitizers (23-bit Digitizer VXI HP E1430A and 24-bit Digitizer NI PXI-5922) were performed. High-quality ADC testing system at the CTU in Prague [5] was applied for this purpose. The input signal was generated by ultra-low distortion Stanford Research DS360 generator and it was subsequently filtered by band-pass filter to achieve high spectral purity of the signal. The record of 2 MSa was divided into four segments. One of them was selected as the reference for calculating coefficients of the inverted polynomial. The other three data segments were then corrected. In the case of VXI HP E1430A digitizer input signal frequency of 20.19 kHz was used. An example of the frequency spectra of the output signal before and after the correction is shown in Fig. 5. The *THD* was improved by about 15 dB by means of the correction.

Secondly, the 24-bit Digitizer NI PXI-5922 was tested. In this case two frequencies of input signal were used: 20.19 kHz and 1.053 MHz. The other conditions remained the same. The residuals before and after the correction show more details than the frequency spectra in this case (see Fig. 6 and 7).

In case of 20 kHz input signal the hysteresis slightly influences the result. The "common mode" non-linearity is well suppressed by the correction but the residual non-linearity of about 15 LSB caused by hysteresis (different for falling and rising slopes) remains. The resulting "common-mode" non-linearity decreased about 20 times.

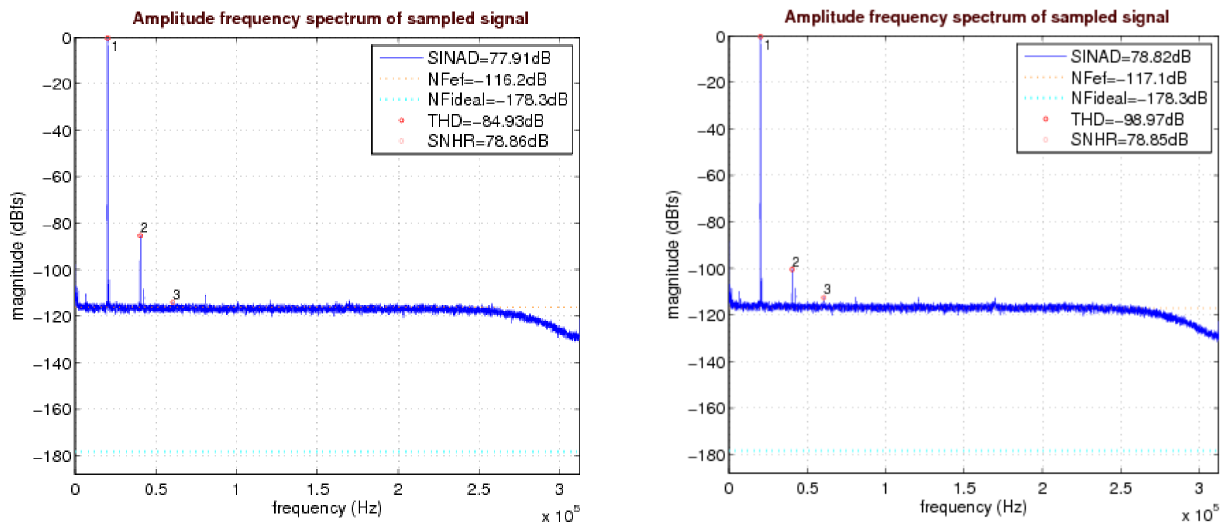

a) Before correction **b) After correction**

Fig. 5 – Frequency spectra of digitized output signal (VXI HP E1430A)

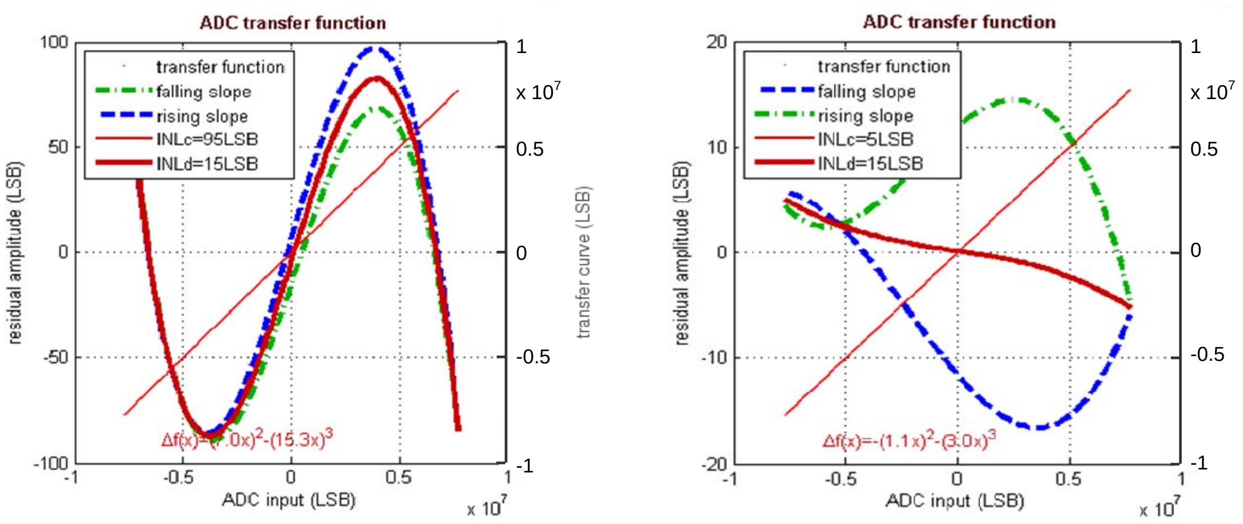

a) Before correction **b) After correction**

Fig. 6 – Integral non-linearity (NI PXI-5922, f_{inp} = 20.19 kHz)

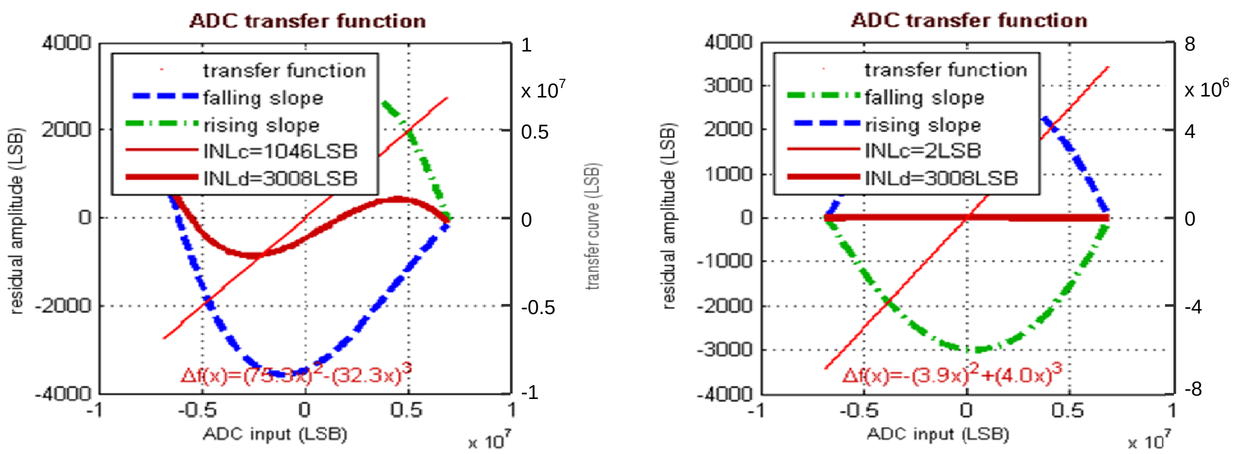

a) Before correction **b) After correction**

Fig. 7 – Integral non-linearity (NI PXI-5922, f_{inp} = 1.053 MHz)

However, for 1 MHz input signal the hysteresis is about two hundreds times higher then for 20 kHz and the "differential-mode" non-linearity caused by the hysteresis is dominant. Common-mode integral non-linearity is suppressed well by the correction indeed but the residual "differential-mode" non-linearity remains and the remaining non-linearity after the correction is practically the same as before.

5. CONCLUSION

Two methods for calculation of coefficients of the inverted polynomial used for ADC non-linearity correction were introduced, derived and compared. The first one uses more straightforward derivation of the coefficients; the second one minimizes the least square error.

The first simulation did not take ADC imperfections (additive noise, jitter in sampling, non-zero sampled signal phase and hysteretic behavior) into account. They showed that the both methods used for calculation coefficients are applicable. Simulations verified that the correction is useable also in the cases when other ADC imperfections are not negligible. This statement was also confirmed experimentally.

The proposed method of ADC non-linearity correction using polynomial approximation of the integral non-linearity $INL(n)$ and its inverse function gives mostly good results but not always. It concerns e.g. digitizers with noticeable hysteresis which is particularly common for signals with frequency near the maximum input frequency of digitizers. Generally, inverse function used for post-correction of INL is frequency dependent. For this reason it cannot be directly used for wide-band signals. However, this issue also concerns other post-correction methods, e.g. look-up table.

6. REFERENCES

[1] *IEEE 1241-2000 Standard for Analog to Digital Converters,* The Institute of Electrical and Electronics Engineers, 2001.

[2] L. Michaeli, P. Michalko, J. Saliga, Fast Gesting of ADC Using Unified Error Model, *The 17th IMEKO world congress*, pp. 534–537, Dubrovnik, Croatia, 2003.

[3] A.C. Serra, M. F. da Silva, P. Ramos, R. C. Martins, L. Michaeli, J. Saliga, Combined Spectral and Histogram Analysis for Fast ADC Testing, *IEEE Transactions on Instrumentation and Measurement*, (54) 4 (2005).

[4] N. Björsell, P. Händel, Achievable ADC Performance by Postcorrection Utilizing Dynamic Modeling of the Integral Nonlinearity", *EURASIP Journal on Advances in Signal Processing*, vol. 2008.

[5] V. Haasz, M. Komarek, J. Roztocil, D. Slepicka, P. Suchanek, System for Testing Middle-Resolution Digitizers Using Test Signal up to 20 MHz, *IMTC/06 Proceedings of the 23th IEEE Instrumentation and Measurement Technology Conference*.

[6] C.L. Monteiro, P. Arpaia, A.C. Serra, A comprehensive phase-spectrum approach to metrological characterization of hysteretic ADCs, *IEEE Transactions on Instrumentation and Measurement*, (51) 4 (2002) pp. 756-763.

[7] P. Suchanek, V. Haasz, D. Slepicka, ADC Nonlinearity Correction Based on INL(n) Approximations. *IEEE International Workshop IDAACS 2009*. Rende, Italy 2009, pp. 137–140.

[8] P. Suchanek, V. Haasz, D. Slepicka, Evaluation of ADC Non-linearity Correction Based on *INL*(*n*) Approximation, *BEC 2012 – 13th Biennial Baltic Electronics Conference* [CD-ROM]. Tallinn, Estonia 2012, pp. 101-104.

Vladimír Haasz*, Head of the Dept. of Measurement of the Czech Technical University in Prague, member of the IMEKO TC-4 – Measurement of Electrical Quantities, member of the IEEE Instrumentation & Measurement Society. He is interested in measurement of dynamic parameters of AD modules including EMC.*

David Slepička*, received the PhD degree in Electrical Engineering in 2005 from the Czech Technical University in Prague. He is currently doing a research on high-resolution ADC testing. The research involves the development of methodologies for analog and digital signal processing and the design of DAQ systems.*

Petr Suchánek *received the PhD degree in Electrical Engineering in 2012 from the Czech Technical University in Prague. The main area of his research concerns the AD converter modelling, results presented here followes from his PhD thesis. Currently, he works for a private company in Czech Aerospace industry.*